YWHAE Influences the Malignant Behaviour of Ovarian Cancer by Regulating the PI3K/AKT and MAPK Pathways Via HE4

Xiao Li
Obstetrics and Gynecology of Shengjing Hospital of China Medical University https://orcid.org/0000-0003-4447-194X

Caixia Wang
Shengjing Hospital of China Medical University

Shuang Wang
Shengjing Hospital of China Medical University

Yuexin Hu
Shengjing Hospital of China Medical University

Shan Jin
Shengjing Hospital of China Medical University

Ouxuan Liu
Shengjing Hospital of China Medical University

Rui Gou
Shengjing Hospital of China Medical University

Xin Nie
Shengjing Hospital of China Medical University

Juanjuan Liu
Shengjing Hospital of China Medical University

Bei Lin (blin@cmu.edu.cn)
Shengjing Hospital of China Medical University https://orcid.org/0000-0002-8881-9859

Primary research

Keywords: YWHAE, HE4, interacting protein, poor prognosis, malignant behaviour, ovarian cancer

Posted Date: April 12th, 2021

DOI: https://doi.org/10.21203/rs.3.rs-385473/v1

Abstract

Background: Malignant tumours of the female reproductive system threaten the lives and health of women worldwide, with ovarian cancer having the highest mortality rate among all malignant tumours. Based on previous work, this study analysed the expression and role of YWHAE in ovarian epithelial tumours.

Methods: The interaction between YWHAE and HE4 was evaluated by immunoprecipitation, western blot analysis, and cellular immunofluorescence. Immunohistochemistry was used to address the relationship between YWHAE expression and clinicopathological parameters and patient prognosis. Changes in cell invasion, epithelial–mesenchymal transition, migration, proliferation, cell cycle, and apoptosis before and after differential expression of YWHAE were also explored in ovarian cancer cell lines and *in vivo* experiments.

Results: YWHAE was found to directly interact with HE4, and its expression was positively correlated with HE4 expression. Moreover, YWHAE higher levels were associated with advanced ovarian cancer cases and with poorer patient outcome. YWHAE was found to enhance the invasion, migration, proliferation, and inhibition of apoptosis of ovarian cancer cells. These biological effects were found to be meditated by the activity of the PI3K/AKT and MAPK signalling pathways.

Conclusions: Altogether, this study demonstrates that YWHAE is significantly increased in ovarian cancer tissues, representing a risk factor for the prognosis of ovarian cancer that is positively correlated with HE4 expression. Furthermore, YWHAE and its downstream signals may represent new therapeutic targets to tackle ovarian cancer.

Introduction

Ovarian cancer has the highest mortality rate among the most common malignant tumours of the female reproductive system. Due to the lack of obvious or specific symptoms, as well as of ideal screening methods, the early detection and diagnosis rates of ovarian cancer are extremely low [1]. When the tumour progresses to an advanced stage, the tumour-free and overall survival times of patients are rapidly shortened [2]. Therefore, it is urgent to find tumour markers with high sensitivity and specificity to guide early clinical screening, early diagnosis, and monitoring of ovarian cancer.

Human Epididymis Protein 4 (HE4) is an ovarian cancer marker that was identified by genomics and proteomics screenings [3]. Its high sensitivity and specificity has attracted the attention of researchers, who have proved that HE4 has more advantages than the common tumour marker CA125 for the early diagnosis of ovarian cancer and for monitoring disease progression [4]. In 2003, HE4 was designated as a serum marker for ovarian cancer and it was approved by the U.S. Food and Drug Administration in 2009 for monitoring the recurrence and progression of epithelial ovarian cancer [5]. Currently, several ongoing clinical studies are addressing the diagnostic potential of HE4, but only few are exploring its underlying molecular mechanisms.

Our previous work has proven that HE4 is highly expressed in ovarian cancer tissues, and that HE4 and Annexin A2 interaction can promote the invasion and metastasis of ovarian cancer. This mechanism is accomplished by activating adhesion signalling pathways such as MAPK and FOCAL [6–7]. Proteins perform their biological functions mainly by interacting with other proteins to form complexes or by working together with chaperone molecules. The tight coordination of proteins with different functions in time and space constitutes the basic process of life. Therefore, given the significant role of HE4 in ovarian cancer, it has become clear that recognition and improved knowledge on HE4-interacting proteins is an important step for an overall better understanding of this disease. A previous study using the two-hybrid screening method and HE4 as bait, has identified the YWHAE protein as a partner of HE4.

Tyrosine 3-monooxygenase/tryptophan 5-monooxygenase activation protein epsilon (YWHAE, also known as 14-3-3ε) belongs to the YWHA protein family, which comprises at least seven highly conserved subtypes of soluble acidic proteins encoded by different genes, namely β, ε, η, γ, τ, ξ, and σ [8]. They can be widely combined with other proteins such as kinases, phosphatases, transmembrane receptors, and transcription factors, among other target proteins [9–11], functioning as a protein interaction bridge in a wide range of biological processes [12–14].

X-ray diffraction analysis showed that YWHAE protein monomers form homodimers or heterodimers [15], which are bound by some highly conserved hydrophobic amino acids. Different YWHA subtypes can bind to the same target, granting these proteins the ideal conditions to regulate a large number of physiological processes, such as cell proliferation, apoptosis, protein transport, metabolic regulation, signal transduction, among others [16–17]. The particular structure of YWHAE may be the basis for its role as a "bridge protein", as well as for its contribution towards disease incidence [18].

Based on previous preliminary findings, this study explored the relationship between YWHAE and HE4 and analysed the expression of YWHAE in ovarian epithelial tumors and its mechanism of action. Enhanced knowledge on the underlying activity of YWHAE and HE4 may provide a basis to further explore the development and progression of ovarian cancer and develop new diagnostic strategies.

Materials And Methods

Primary samples

Ovarian tissue samples were derived from paraffin specimens surgically collected between 2008 and 2012 in the Department of Obstetrics and Gynecology, Shengjing Hospital, China Medical University. A total of 16 samples were derived from normal ovarian tissue removed due to uterine fibroids or cervical cancer (normal group), 18 samples were from benign cases, 24 samples were classified as borderline, and 105 samples were from malignant ovarian cancers. The pathological types among the malignant samples included 71 serous tumours, 7 mucinous tumours, 19 endometrioid tumours, and 8 clear cell carcinomas. The malignant group was also classified according to pathology assessment, with 51 cases identified as highly differentiated and 54 as poorly differentiated. The surgical pathological staging was performed in accordance with the International Union of Obstetrics and Gynecology (FIGO) standards: 44

cases in stage I-II and 61 in stage III-IV, of which a comprehensive exploratory operation was performed in the early stage and cytoreductive surgery was performed in the late stage. In the malignant group, 92 patients underwent lymph node dissection, with lymph node metastasis being confirmed in 28 cases. Protein samples for western blotting analysis were derived from tissue specimens collected in 2018–2019 in the Department of Obstetrics and Gynecology, Shengjing Hospital Affiliated to China Medical University. A total of 33 specimens were surgically collected from 15 cases in the malignant group, 6 cases in the borderline group, 6 cases in the benign group, and 6 cases in the normal group. All cases were newly diagnosed and radiotherapy and chemotherapy naïve.

Immunochemistry

The histopathological specimens were fixed with 10% formalin solution, embedded in paraffin, and then serially sectioned into 5 μm slices. The paraffin sections were deparaffinised with xylene and re-hydrated with gradient alcohol solutions, and the antigens were hot-recovered. Then, H_2O_2, goat serum blocking solution, and an anti-YWHAE antibody (1:100, sc-23957, Santa Cruz Biotechnology, Santa Cruz, CA) or an anti-HE4 (1:1500, ab200828, Abcam, Cambridge, UK) antibody were added dropwise sequentially, and the solutions were left to incubate overnight at 4 °C. On the next day, the slices were incubated in horseradish peroxidase (HRP)-labelled goat anti-rabbit/mouse secondary antibodies and stained using 3,3-diaminobenzidine (Ultrasensitive TM SP Mouse/Rabbit IHC Kit, Maixin, Fuzhou, China). The cell nucleus was stained blue using haematoxylin. The sections were then dehydrated, cleared by xylene, and mounted.

The results were evaluated by two pathologists who did not know in advance the clinical information of the patients, and they independently observed and scored each sample. If discordant scoring results were obtained, a third pathologist would assess the sample for the final decision. The samples were classified as positive when presenting with brownish-yellow or brown colour in the cell cytoplasm and/or membrane. If the proportion of positive cells was less than 5%, it was scored as 0 points, 5–25% was scored as 1 point, 26–50% was 2 points, 51–75% was 3 points, and more than 75% was counted as 4 points. According to the colour intensity, they were further scored with 3 points for brown, 2 points for brownish-yellow, 1 point for light yellow, and 0 points for no staining. To reach a final score, the two classifications were multiplied: 0–2 points were recorded as negative expression (−), 3–4 points as weak positive expression (+); 5–8 points as moderate positive expression (++), and 9–12 points as strong positive expression (+++).

Cellular immunofluorescence

The cells were seeded on a microscope slide and washed with PBS after they adhered to the glass. Goat serum blocking solution was added, followed by the anti-YWHAE (1:100, sc-23957, Santa Cruz Biotechnology, Santa Cruz, CA) and anti-HE4 (1:200, DF8160, Affinity, OH, USA) primary antibody mix. A secondary antibody mixture containing tetramethylrhodamine-labelled goat anti-rabbit IgG (SA00007-2, Proteintech, Wuhan, China) and fluorescein isothiocyanate-labelled goat anti-mouse IgG (SA00003-1,

Proteintech, Wuhan, China) was dropped onto the slide, which was then incubated for 2 h in the dark. 4',6-diamidino-2-phenylindole (4083S; Cell Signaling Technology, Beverly, MA, USA) was used to stain the cell nucleus, and an anti-quenching agent was added dropwise onto the slide immediately before assessing the slices on a confocal microscope.

Establishment of stable over-expressing YWHAE cell lines and transient YWHAE-knockdown cell lines

The ovarian cancer cell lines CAOV3 and ES2 (Institute of Biochemistry and Cell Biology, Chinese Academy of Sciences, Shanghai, China) were cultured in RPMI 1640 medium (Biological Industries, Beit-Haemek, Israel) containing 10% foetal bovine serum (Biological Industries, Beit-Haemek, Israel). When the cells reached 80–90% confluence, the medium was discarded, the cells were washed with phosphate-buffered saline (PBS), trypsinised, and split to continue the culture.

YWHAE-siRNA and *HE4*-siRNA were transfected into CAOV3 and ES2 cells. *YWHAE*-siRNA (GAAGCAGGUUAGCGUUGAATTUUCAACGCUAACCUGCUUCTT), *Mock-YWHAE*-siRNA (GAAGCAGGUUAGCGUUAGATTUU), *HE4*-siRNA (UUCUCCGAACGUGUCACGUTTACGUGACACGUUCGGAGAATT), and *Mock-HE4*-siRNA (UUCUCCGAACGUGUACGUTT) working solutions were prepared according to the manufacturer's instructions (Gene Pharma, Suzhou, China). The cells were seeded in 6-well plates with serum-free medium on the day of transfection. The transfection was performed using Lipofectamine 3000 (Invitrogen, Waltham, MA, USA) according to the manufacturer's instructions.

Lentivirus-mediated *YWHAE* over-expression vector was used to transfect OVCAR3 and A2780 cell lines, which had relatively low expression of YWHAE. To calculate the multiplicity of infection (MOI) of YWHAE-expressing lentivirus, 500 μL of complete medium were added to a 24-well plate, in addition to lentivirus supernatant and a corresponding volume of polybrene, to promote transfection. Puromycin at 50% lethal concentration (LC50) was used to select the efficiently transfected cells.

Western blotting

Total protein samples were separated by sodium dodecyl sulphate polyacrylamide gel electrophoresis. Briefly, 5–10 μL of protein sample was placed on each well of the gel and subjected to 80–120 V of constant electrical current for 40–100 min. The proteins were transferred onto a polyvinylidene fluoride membrane (Millipore, Burlington, MA, USA), which was then blocked with 5% milk/bovine serum albumin solution for 2 h at 37 °C. The membrane was incubated overnight at 4 °C with primary antibodies (YWHAE, 1:1000, ab92311, Abcam, Cambridge, UK; HE4, 1:1500, DF8160, Affinity, OH, USA; Cyclin D1, 1:1000, 2978S,Cell Signaling Technology, Beverly, MA□Ki-67, 1:1000, 9449S, Cell Signaling Technology, Beverly, MA; Bax, 1:1000, 5023S, Cell Signaling Technology, Beverly, MA; Bcl-2, 1:1000, 12789-1-AP, Proteintech, Wuhan, China; MMP2, 1:1000, 10373-2-AP, Proteintech, Wuhan, China; MMP9, 1:1000, 10375-2-AP, Proteintech, Wuhan, China□E-cadherin, 1:1000, 20874-1-AP, Proteintech, Wuhan, China; N-cadherin, 1:1000, 4061S, Cell Signaling Technology, Beverly, MA; Vimentin, 1:3000, 10366-1-AP, Proteintech, Wuhan, China; PI3K, 1:1000, 4292S, Cell Signaling Technology, Beverly, MA; p-PI3K, 1:1000, 4228S, Cell Signaling

Technology, Beverly, MA; AKT, 1:1000, 4691S, Cell Signaling Technology, Beverly, MA; p-AKT, 1:1000, 4060S, Cell Signaling Technology, Beverly, MA; m-TOR, 1:1000, 2972S, Cell Signaling Technology, Beverly, MA; p-m-TOR, 1:1000, 2971S, Cell Signaling Technology, Beverly, MA; MEK, 1:1000, sc-81504, Santa Cruz Biotechnology, Santa Cruz, CA□p-MEK, 1:1000, 2338S, Cell Signaling Technology, Beverly, MA; ERK, 1:1000, 9102S, Cell Signaling Technology, Beverly, MA; p-ERK, 1:1000, 9101S, Cell Signaling Technology, Beverly, MA). After washing, the membrane was incubated with HRP-labelled goat anti-rabbit (1:3000, ZB-2301, ZSGB-BIO, Beijing, China) or goat anti-mouse (1:3000, ZB-2305, ZSGB-BIO, Beijing, China) secondary antibodies for 1 h at 37℃ and then washed again. Lastly, western chemiluminescent HRP Substrate (Thermo Fisher Scientific, Waltham, MA, USA) was added dropwise onto the membrane, and luminescent signals were detected in a luminometer at different exposure times.

Immunoprecipitation

Cells in exponential growth were collected and washed. Iced lysis buffer was added and the cell suspension was sonicated. The supernatant was collected and total protein concentration was determined. Total protein samples (500 μg) were incubated with 2 μg of YWHAE (1□100, sc-23957, Santa Cruz Biotechnology, Santa Cruz, CA) or HE4 (1:1500, ab200828, Abcam, Cambridge, UK) primary antibody. An IgG antibody (5145S, Cell Signaling Technology, Beverly, MA) of the same species of the primary antibody was used as negative control. After mixing, the samples were left overnight at 4°C with slow rotation. Afterwards, beads (sc-2003, Santa Cruz Biotechnology, Santa Cruz, CA) were added to each tube and incubated for 6 h. The bound proteins were collected by centrifugation, (2×) Loading Buffer was added, and the samples were heated to denature the proteins.

Invasion test

A transwell insert was placed in the culture plate. Matrigel (1:7.5 dilution, 356234, BD Biosciences, New York, USA) and serum-free 4×10^4 cell suspension were added to the upper layer of the chamber, whereas the lower chamber contained complete medium (with serum). After culturing for 48–72 h, the cells in the lower chamber were collected, fixed, and stained. Residual cells lefts on plate were observed under a microscope. The experiment was repeated thrice.

Scratch test

Cells were seeded in a 6-well culture plate and maintained at 37 °C in a 5% CO_2 incubator. After confirming under the microscope that the cells were at 90% confluence, the cell layer was scratched with a 100 μl pipette tip. The cells were cultured in serum-free medium for 24 h, then washed with PBS and photographed to monitor the healing of the scratches. The experiment was repeated thrice.

MTT assay

A total of 2,000 cells/well were seeded in a 96-well culture plate and maintained at 37 °C in a 5% CO_2 incubator. After the cells were adhered, 20 μL of sterile MTT (M8180, Solarbio, Beijing, China) working

solution was added to each well, mixed well, and the cells were incubated at 37 °C for 4h. Following this, the medium was aspirated and 150 μL of DMSO (D8370, Solarbio, Beijing, China) was added to each well. The absorbance of each well was measured in a microplate reader after shaking for 5 min. The experiment was repeated thrice.

Cell cycle analysis

Cells in log phase were collected and washed, and pre-cooled ethanol was slowly added to fix the cells for later use. Before the analysis, a totle of 500 μl PI/ RNase A (KGA512, KeyGen Biotech, Nanjing, China) staining solution were added to the cell suspension and the cells were left in the dark for 20 min, according to the manufacturer's instructions. The cells were analysed by flow cytometry. The experiment was repeated thrice.

Apoptosis assessment

The Annexin V/PI double staining method was used to evaluate the impact of YWHAE overexpression on ovarian cancer cells. The cells were trypsinized without EDTA, and the suspension was centrifuged to discard the supernatant. The cells were re-suspended in 500 μL of Binding Buffer added slowly and incubated with 5 μL of Annexin V-APC (550474, BD Biosciences, New York, USA) / FITC (KGA107, KeyGen Biotech, Nanjing, China) and PI in the dark at 37 ℃ for 15 minutes according to the manufacturer's instructions. The staining was evaluated by flow cytometry.

In vivo xenograft model of ovarian cancer

Twenty female nude mice (Huafukang Biosciences, Beijing, China) were randomly divided into two groups and injected with either OVCAR3-YWHAE-MOCK or OVCAR3-YWHAE-H ovarian cancer cell lines. Approximately 100 μL of cell suspension containing 1×10^7 cells was injected subcutaneously into the armpit of the right forelimb of each nude mouse. The tumour progression and overall health status of the mice were observed every three days, and the diameter of the tumour and the weight of the mice were measured. The tumour volume was calculated as $V = (a \times b^2)/2$, where a represents the largest diameter and b the shortest diameter. On day 7 post-injection the newly formed tumours were detectable, while on day 21 the largest tumour was nearly 1 cm in diameter, and the mice had started to shown poor health symptoms.The tumor samples were then fixed in 4% paraformaldehyde and embedded in paraffin. Continuous 5 μm-thick sections were cut and analyzed using hematoxylin and eosin (HE) or immunohistochemical staining. The animal study was approved by the Institutional Animal Research Committee of China Medical University.

Signalling pathway inhibition experiment

YWHAE-overexpressing and mock-transduced cells were cultured in the presence of the phosphatidylinositol-4,5-bisphosphate 3-kinase (PI3K) inhibitor (GDC-0941, Selleck, Houston, USA), or a

selective inhibitor of mitogen-activated protein kinase 1 and 2 (MAPK1/2) inhibitor (PD98059, Selleck, Houston, USA), 25 and 20 μmol/L, respectively. 0.1% DMSO served as the negative control.

Bioinformation analysis

The YWHAE co-expression gene set was downloaded from cBioPortal (www.cbioportal.org), and the top 300 genes were annotated according to the gene ontology (GO) (BP, biological process; CC, cellular component; and MF, molecular function) and the Kyoto Encyclopaedia of Genes and Genomes (KEGG) pathway analysis using the tools available in DAVID (www.david.ncifcrf.gov). The interaction network among the top 100 genes was constructed using STRING (www.string-db.org) and Cytoscape (www.cytoscape.org).

The Oncomine database (http://www.oncomine.org), which is currently the world's largest oncogene chip database integrated with a data mining platform, was used to analyze the mRNA expression level of YWHAE in the different cancer cell types.

The protein-protein interaction (PPI) network was constructed using the STRING (http://string.embl.de/) online tool. The visualization plot was generated using Cytoscape software with a confidence score of ≥0.1 defined as the cutoff. The core modules of the PPI network were screened using Molecular Complex Detection (MCODE) with the following parameters: degree threshold = 2, node threshold = 0.2, kcore = 2, and maximum depth = 100.

Statistical analysis

Statistical differences between two groups were evaluated by the Student's *t* test, and one-way analysis of variance was used for the comparison of more than two groups. The data were counted using the χ^2 and Fisher's exact probability tests, and measurements of the data were performed using the single factor analysis of variance. $P<0.05$ was considered statistically significant.

Results

YWHAE and HE4 are interacting proteins in ovarian cancer

The levels of YWHAE and HE4 were evaluated in the CAOV3 and ES2 ovarian cancer cell lines by cellular immunohistochemistry, revealing that both proteins were expressed in the cytoplasm and cell membrane (Fig. 1a). Co-localizing in the cytoplasm and cell membrane of CAOV3 and ES2 (Fig. 1b). Co-immunoprecipitation of both YWHAE and HE4 in these cell lines further demonstrated that they are interacting proteins (Fig. 1c), siRNA-mediated knock-down of *YWHAE* led to reduced levels of HE4 in both CAOV3 and ES2 transiently transfected cells, whereas *HE4* knock-down had no significant effect on YWHAE levels. These results suggest that YWHAE is upstream of HE4 (Fig. 1d) and it can regulate HE4 expression.

David analyzed the GO (BP/CC/MF) and KEGG pathways of the top 300 gene set, and enriched 36 BP, such as RNA scattering, Wnt signaling pathway, cell adhesion, 23 CC, 13 MF (all $P<0.05$), and 2 KEGG signaling pathways (all $P<0.05$), such as spliceosome, RNA transport, etc., and drew the bubble diagram of the top 5 go (BP/cc/MF) and KEGG pathways. The results showed that YWHAE might interact with PAFAH1B1, EIF5A, PITPNA, TIMM22, PFN1, WFDC2(HE4) (Fig. 1e).

The expression and correlation analysis of YWHAE and HE4 in each group of ovarian tissue

YWHAE expression in ovarian tissues

In agreement with the cell line results, analysis of primary tissue samples showed that YWHAE was mainly located in the cytoplasm and cell membrane. Approximately 96.19%[101/105] of the malignant samples were positive for YWHAE with a strong positive rate of 70.48%[74/105], whereas the borderline group had a YWHAE-positive rate of 41.67%[10/24] and a strong positive rate of 16.67%[4/24]. Benign and normal ovarian samples had a positive rate of 16.67%[3/18] and 6.25%[1/16], and a strong positive rate of 11.11%[2/18] and 0.00%[0/16], respectively. Comparison between the different groups revealed that YWHAE-positive expression was significantly higher in the malignant group ($P<0.05$); however, the junction group YWHAE-positive rate was also higher than that of the benign and normal groups ($P<0.05$). The expression rate of YWHAE in the benign group was higher than in the normal group, but the difference was not statistically significant ($P>0.05$) (Table 1, Fig. 2a,b)

Relationship between YWHAE expression and clinicopathological parameters of ovarian cancer

In order to compare clinicopathological parameters with the expression of YWHAE in ovarian tissue, we reviewed the clinical information of the 105 patients with primary ovarian epithelial malignant tumours. Analysis of the pathological data showed that YWHAE-strong positive expression rate was significantly higher in FIGO III-IV stage ovarian epithelial malignancies than in the early stage group (80.33% versus 56.82%, $P<0.01$). No statistical differences were observed in their other clinicopathological parameters (Table 2, Fig. 2c).

Relationship between YWHAE expression and survival prognosis of patients with ovarian cancer

Follow-up of the patients further showed that only four deaths occurred in the YWHAE low expression group (n=31), while 21 deaths were recorded in the YWHAE high expression group (n=74). Kaplan-Meier survival analysis showed that the survival rate among patients with high YWHAE levels was significantly lower compared with that in the YWHAE low expression group. This result followed the same trend as observed when comparing patients with early or late FIGO staging ($P<0.05$) (Fig. 2d). Univariate and multivariate Cox regression analysis of YWHAE expression with age, pathological type, degree of differentiation, FIGO stage, and lymph node metastasis demonstrated that YWHAE expression and FIGO staging are risk factors for the prognosis of epithelial ovarian malignancies (Fig. 2e).

YWHAE and HE4 expressions are related in ovarian cancer tissues

Next, the co-expression of YWHAE and HE4 was evaluated in 80 cases of ovarian cancer. A total of 0, 3, 9, and 68 cases were YWHAE−/HE4−, YWHAE−/HE4+, YWHAE+/HE4−, and YWHAE+/HE4+, respectively. Spearman correlation analysis confirmed that YWHAE and HE4 expressions are positively correlated in ovarian cancer (correlation coefficient Rs=0.277, *P*=0.013) (Table 3). Linear regression analysis showed that the expression of YWHAE and HE4 can influence each other (*P*<0.05), and that the late FIGO stage is an important factor affecting the expression of HE4 (Table 4). Multivariate linear regression analysis also showed that HE4 expression score was an independent influencing factor of YWHAE expression, as well as YWHAE expression was an independent influencing factor of HE4 expression (Fig. 2e).

YWHAE and HE4 expressions are related in ovarian cancer tissues

Study of YWHAE expression in Oncomine database showed that YWHAE was highly expressed in the many cancer group compared to the normal tissue group, for ovarian cancer, YWHAE was significantly highly expressed in 185 ovarian carcinoma tissues compared with 10 ovarian surface epithelium tissues (Fig. 2g,h).

YWHAE promotes ovarian cancer cell invasion, migration, and epithelial–mesenchymal transition potential

Analysis of the levels of YWHAE in several ovarian cancer cell lines revealed that it was higher in CAOV3 and ES2 than in OVCAR3 and A2780. Based on these results, CAOV3 and ES2 cells with relatively high expression of YWHAE were used to establish a cell line model with low YWHAE expression, whereas OVCAR3 and A2780 ovarian cancer cells with relatively low YWHAE were used to establish a stable over-expressing cell line model of YWHAE (Fig. 3a-f).

The effect on invasion and migration of ovarian cancer cells upon transient knock-down or stable over-expression of YWHAE was evaluated next by transwell and scratch experiments. Overall, the data revealed that both OVCAR3 and A2780 cells overexpressing YWHAE had significantly enhanced invasion and migration capacity than mock-transduced and untransduced cells. In contrast, CAOV3 and ES2 cells lacking YWHAE showed weaker invasion and migration abilities compared with control cells (all P<0.05) (Fig. 3g-n). To further explore the impact of YWHAE on the behaviour of ovarian cancer cells, the levels of cell epithelial and mesenchymal markers were evaluated in these cells by western blot. YWHAE-overexpression was found to be associated with higher levels of the N-cadherin, Vimentin, MMP2, and MMP9 (cell mesenchymal markers), whereas the epithelial marker E-cadherin was found to be reduced compared with that of cells of the control groups. The opposite trend was seen when YWHAE was knocked-down (both *P*<0.05), with higher levels of E-cadherin and reduced levels of N-cadherin, Vimentin, MMP2, and MMP9 (Fig. 4a-d). Altogether, these results demonstrate that YWHAE promotes invasion, migration, and epithelial-mesenchymal transition of epithelial ovarian cancer cells.

YWHAEpromotes ovarian cancer via inducing cell proliferation, cell cycle progression, and apoptosis inhibition

Additional assessment of the OVCAR3 and A2780 YWHAE-over-expressing cells further showed that more of these cells were in G2/M phase, suggesting that they were actively proliferating compared with mock-transduced and untransduced cells (all $P<0.05$). Furthermore, these cells had higher expression of Ki67, Cyclin D1, and Bcl-2 and reduced levels of Bax (all $P<0.05$). CAOV3 and ES2 cells lacking YWHAE showed the opposite results, with significantly lower proportion of cells in the G2/M phase, reduced levels of proliferation markers, and increased levels of the Bax apoptosis marker. Furthermore, flow cytometry results revealed that compared with the control group, the overall apoptosis of OVCAR3 and A2780 cells was significantly reduced after YWHAE overexpression ($P<0.05$) , while apoptosis was significantly increased in OVCAR3 and A2780 cells compared to the control group when YWHAE expression was inhibited (Fig. 4e-h, Fig. 5). Taken together, these results demonstrate that the expression of YWHAE can enhance the proliferation of ovarian cancer cells, while it also promotes cell cycle progression and inhibits cell apoptosis.

Effect of YWHAE on the in vivo tumorigenesis of ovarian cancer cells

In order to explore the effect of YWHAE on the tumorigenic ability of ovarian cancer cells, OVCAR3 stably overexpressing YWHAE or a mock control were injected into athymic nude mice. Assessment of the tumours formed 21 days after the cells were injected revealed that cells overexpressing YWHAE were significantly bigger and weighed about 2.83 times more than the tumours seen in the control group. Moreover, the growth rate of the tumours produced by YWHAE-overexpressing cells was also significantly higher compared with those in the control group (Fig. 6a-c). Tumour biopsies collected and evaluated by immunohistochemistry revealed that the signals of activated AKT and ERK (p-AKT and p-ERK, respectively) were stronger in OVCAR3 cells over-expressing YWHAE, further suggesting that YWHAE can promote the proliferation of tumour cells *in vivo* (Fig. 6d).

YWHAE-induced cellular effects are mediated by the PI3K/AKT and MAPK signalling pathways

We used the STRING database to predict the relevant molecules of YWHAE by PPI, and the results showed that YWHAE had direct or indirect interaction with PI3K, MAPK, ACTR1A, cAMP-dependent protein kinase and other molecules (Fig. 7a).

To have a more detailed perspective on the underlying mechanisms triggered by YWHAE, the levels of several critical signalling molecules were evaluated by western blotting. The results showed that the ratio of p-PI3K/PI3K, p-AKT/AKT, mTOR/p-m-TOR, p-ERK/ERK, and p-MEK/MEK increased significantly in the presence of high levels of YWHAE, but they were reduced upon YWHAE-knock-down (all $P<0.05$). The above results prove that YWHAE can activate PI3K/AKT and MAPK signal pathways (Fig. 7b-e).

To further explore the role of these two signalling pathways on YWHAE-induced cellular effects, PI3K inhibitor (GDC-0941) or MEK inhibitor (PD98059) was used. The invasion and migration experiments were repeated in the presence of these chemical inhibitors, revealing that blockage of both PI3K/AKT and MAPK signals significantly weakened the pro-invasion and pro-migration effect promoted by YWHAE over-expression ($P<0.05$). Moreover, the results of the MTT experiment showed that the proliferation

ability of OVCAR3 cells overexpressing YWHAE-H was significantly reduced in the presence of GDC-0941 or PD98059 (P<0.05) (Fig. 8, Fig. 9).

The above described results demonstrate that YWHAE can impact on the invasion, migration, and proliferation potentials of ovarian cancer cells, as well as other malignant biological behaviours, through the PI3K/AKT and the MAPK signalling pathways.

Discussion

Ovarian cancer is the tumour of the female reproductive system with the highest mortality rate. Although a variety of targeted drugs for ovarian cancer have been used in the clinical setting, its high mortality rate still represents a serious threat to the lives and health of women worldwide.

YWHAE protein is widely expressed in eukaryote cells, and has been detected in wheat [19], giant trematodes in goat blood cells [20], liver flukes [21], and mosquitoes [22]. Moreover, in the physiological state of the human body, YWHAE was described as an important element in retinal photoreceptor rod cells [23]. Some researchers have found that YWHAE is also involved in the differentiation of adipose-derived mesenchymal stem cells into osteoblasts, enhancing the body's osteogenic ability [24]. In contrast, some studies have detected a peak of YWHAE expression 168 h after partial liver resection, preventing cell cycle and negatively regulating liver regeneration [25]. Therefore, these discordant findings suggest that YWHAE may have a two-way regulatory effect on the cell cycle.

Since YWHAE was originally identified in the brain, its pathological effects were initially investigated in the field of neurological diseases, such as Parkinson's [26] and Alzheimer's disease [27], brain excitotoxic injury [28], and myocardial ischemia reperfusion [29], among others. These studies agreed that the mechanism by which YWHAE could impact on nerve cells could be related to mitochondrial dysfunction and regulation of apoptosis.

In recent years, studies have suggested that abnormal expression of YWHAE may also play an important role in the occurrence and development of tumours. Liang et al. found that YWHAE is highly expressed in kidney cancer tissues, and *in vitro* experiments demonstrated that YWHAE can promote the abnormal proliferation of tumour cells [30]. In gastric cancer cell lines, the expression of YWHAE is significantly increased and it can inhibit cell proliferation, invasion, and migration by reducing the expression of MYC and CDC25B, whereas MYC induces cell proliferation, invasion, and migration by enhancing CDC25B and reducing YWHAE expression [31–32]. In breast cancer, YWHAE expression was also related to tumour size, lymph node metastasis, and patient survival prognosis, as well as to breast cancer cell resistance to chemotherapy. Indeed, YWHAE overexpression significantly increases breast cancer cell proliferation, migration, and invasion, whereas reduced YWHAE expression prevents Snail and Twist expression in breast cancer cells [33]. Although high expression of YWHAE has been described in colorectal, liver, kidney, breast, gastric, and oesophageal cancers, its specific mechanism of action remains unclear. Among the malignant tumours of the female reproductive system, YWHAE is more commonly reported upon genetic testing of the uterine sarcoma cells. Endometrial stromal sarcoma carrying the YWHAE–

NUTM2 (or YWHAE–FAM22) fusion gene has obvious malignant biological effects, such as enhanced invasion and drug resistance, and the prognosis of patients harbouring such genetic abnormality is worse [34–35]. Sylvain et al. [36] performed gene chip detection on matched tumour samples from six patients with advanced high-grade epithelial ovarian cancer before and after chemotherapy. The results showed that 54 genes that recurred after chemotherapy showed a down-regulation trend, whereas 121 genes, including *YWHAE*, showed an up-regulation trend. This change in the expression profile suggests that YWHAE may be related to ovarian cancer invasion, proliferation, and drug resistance. Sun et al. used the Gene Expression Omnibus database to analyse the relationship between ovarian cancer and diabetes, finding that 10 key genes, including *YWHAE*, are important links in the regulation of the redox reaction process and carboxylic acid metabolism in the body [37]. Based on these results, they believe that ovarian cancer is related to sugar metabolism, and that certain key metabolism-related genes and proteins could be used as potential targets for the treatment of ovarian cancer.

Altogether, the results described in the present study demonstrate that YWHAE and HE4 are interacting proteins. And YWHAE is significantly associated with advanced stage cancers and poorer patient outcomes, thereby speculating that high YWHAE expression may represent a risk factor for the prognosis of ovarian cancer. Overall, YWHAE showed a similar cancer-promoting effect as seen with HE4, partaking in the occurrence and development of ovarian cancer.

Through induced differential expression of YWHAE and *in vivo* experiments, it was also demonstrated that YWHAE contributes to ovarian cancer cell invasion, epithelial-mesenchymal transition, and migration, as well as to enhancing their proliferative and anti-apoptotic responses.

Previous studies have confirmed that HE4 mainly plays an important role in the spreading and adhesion of ovarian cancer cells. Moreover, low levels of HE4 prevented the activation of ERK and EGFR in ovarian cancer cells. Therefore, it is believed that HE4 may influence the biological behaviour of cancer cells in the ovaries through the EGFR and MAPK signalling pathways, but the specific underlying mechanism is still unclear. Studies have reported that HE4 can affect the cell cycle (G0/G1 phase), migration, and invasion capabilities by regulating the ERK/MAPK signals and the expression of MMP-9, MMP-2, and cathepsin B [38]. In accordance with its role as an interaction protein of HE4, YWHAE was also shown to affect the malignant biological behaviour of ovarian cancer cells through the above-mentioned signalling pathways.

In breast cancer, YWHAEτ acts together with 1,3-DCQA (eicosanylquinic acid) to prevent the proliferation and metastasis of cancer cells through the Jak/PI3K/AKT and Raf/ERK pathways and by inducing the Bad/Bax/caspase 9 apoptosis pathway [39]. Overexpression of YWHAEζ can regulate the expression of Snail protein by activating PI3K/AKT signals, thereby significantly promoting the proliferation, migration, and invasion of glioma cells, representing a potential prognostic marker therapeutic target for glioma [40]. In colorectal cancer, YWHAEσ acts as a tumour suppressor gene. However, COPS5 and LASP1 through PI3K/AKT-dependent signals stimulate YWHAEσ ubiquitination and degradation, making it lose its tumour suppressor activity, thereby promoting the progression of colorectal cancer [41].

Relevant studies have shown that YWHAE can inhibit cell apoptosis in colorectal cancer HT-29 cells [42], and this process can be reversed by non-steroidal anti-inflammatory drugs. The inhibition of apoptosis may be related to the ability of YWHAE to interfere with mitochondrial pro-apoptotic mechanisms and activate the transcription factors FKHRL1 and Bad [43]. Moreover, ATPR (4-amino-2-trifluoromethyl-phenylretinoic acid) can induce G0/G1 phase arrest in gastric cancer SGC-7901 cells by down-regulating YWHAE [44]. We found that PI3K/AKT pathway node proteins (PI3K, AKT, and mTOR) and MAPK pathway node proteins (MEK and ERK) were significantly activated in ovarian cancer cells over-expressing YWHAE. Importantly, inhibition of these pathways with specific inhibitors prevented the pro-invasion, pro-migration, and pro-proliferation effects induced by YWHAE. Therefore, these results suggest that YWHAE promotes the malignant biological behaviour of epithelial ovarian cancer through activation of the PI3K/AKT and MAPK pathways.

Conclusions

This study described for the first time that YWHAE and HE4 were interacting proteins and underlying a co-localization relationship. It was proved in tissues that the expression of YWHAE was significantly increased in ovarian cancer tissues, which was a risk factor for the prognosis of ovarian cancer. Moreover, it was discovered for the first time that YWHAE could promote the invasion, migration, proliferation of epithelial ovarian cancer through PI3K/AKT and MAPK pathways. In the future, YWHAE may be used as a prognostic factor and trigger new research ideas for further understanding the underlying pathogenesis and improving the diagnosis and treatment of ovarian cancer.

Abbreviations

HE4	Human Epididymis Protein 4
FIGO	International Union of Obstetrics and Gynecology
GSEA	Gene Set Enrichment Analysis
FBS	Fetal bovine serum
DMSO	dimethyl sulfoxide
COIP	Co-Immunoprecipitation
FITC	Fluorescein isothiocyanate
TRITC	Tetramethylrhodamine-5-isothiocyanate
DAPI	4',6-diamidino-2-phenylindole
PBS	phosphate-buffered saline
PVDF	polyvinylidene fluoride membrane
KEGG	Kyoto Encyclopedia of Genes and Genomes
GO	Gene Ontology

Declarations

Availability of data and materials

Not applicable.

Acknowledgements

We would like to acknowledge the reviewers for their helpful comments on this paper.

Funding

The study was supported by grants from the National Natural Science Foundation of China (81672590 and 81472437) and Shengjing Freedom Researchers' plan (201804).

Author information

Affiliations

Department of Obstetrics and Gynaecology, Shengjing Hospital Affiliated to China Medical University, No. 36, Sanhao Street, Heping District, Shenyang, 110004, People's Republic of China.

Xiao Li, Caixia Wang ,Shuang Wang, Yuexin Hu, Shan Jin, Ouxuan Liu, Rui Gou, Xin Nie, Juanjuan Liu, Bei Lin.

Contributions

XL and BL finished study design, CW, SW, YH, SJ, OL, RG finished experimental studies, XN, JL finished data analysis, XL finished manuscript editing. All authors read and approved the final manuscript.

Corresponding author

Correspondence to Bei Lin.

Ethics declarations

Ethics approval and consent to participate.

This study was approved and supervised by the animal ethics committee of Shengjing Hospital Affiliated to China Medical University. The treatment of animals in all experiments conforms to the ethical standards of experimental animals.

Consent for publication

Not applicable.

Competing interests

The authors declare that they have no conflicts of interest.

References

1. Chen W. Cancer statistics: updated cancer burden in China. Chin J Cancer Res. 2015;27(1):1.
2. Jelovac D. Armstrong DK. Recent progress in the diagnosis and treatment of ovarian cancer. CA Cancer J Clin. 2011;61(3):183–203.
3. Kirchhoff C. Molecular characterization of epididymal proteins. Rev Reprod. 1998;3(2):86–95.
4. Huang J. Chen J, Huang Q. Diagnostic value of HE4 in ovarian cancer: A meta-analysis. Eur J Obstet Gynecol Reprod Biol. 2018;231:35–42.
5. Dochez V. Caillon H, Vaucel E. Dimet J, Winer N. Ducarme G. Biomarkers and algorithms for diagnosis of ovarian cancer: CA125, HE4, RMI and ROMA, a review. J Ovarian Res. 2019;12(1):28.
6. Wang J. Deng L, Zhuang H. Liu J, Liu D. Li X, *et al.* Interaction of HE4 and ANXA2 exists in various malignant cells-HE4-ANXA2-MMP2 protein complex promotes cell migration. Cancer Cell Int. 2019;19:161.
7. Zhuang H. Tan M, Liu J. Hu Z, Liu D. Gao J, *et al.* Human epididymis protein 4 in association with Annexin II promotes invasion and metastasis of ovarian cancer cells. Mol Cancer. 2014;13:243.
8. Diallo K. Oppong AK, Lim GE. Can 14-3-3 proteins serve as therapeutic targets for the treatment of metabolic diseases? Pharmacol Res. 2019;139:199–206.

9. Cau Y. Valensin D, Mori M. Draghi S, Botta M, Structure. Function, Involvement in Diseases and Targeting of 14-3-3 Proteins: An Update. Curr Med Chem. 2018;25(1):5–21.
10. Morrison DK. The 14-3-3 proteins: integrators of diverse signaling cues that impact cell fate and cancer development. Trends Cell Biol. 2009;19(1):16–23.
11. Wilker E. Yaffe MB. 14-3-3 Proteins–a focus on cancer and human disease. J Mol Cell Cardiol. 2004;37(3):633 – 42.
12. Aghazadeh Y. Papadopoulos V. The role of the 14-3-3 protein family in health, disease, and drug development. Drug Discov Today. 2016;21(2):278–87.
13. Hartman AM. Hirsch AKH. Molecular insight into specific 14-3-3 modulators: Inhibitors and stabilisers of protein-protein interactions of 14-3-3. Eur J Med Chem. 2017;136:573 – 84.
14. Kaplan A. Morquette B, Kroner A. Leong S, Madwar C. Sanz R, *et al.* Small-Molecule Stabilization of 14-3-3 Protein-Protein Interactions Stimulates Axon Regeneration. Neuron. 2017;93(5):1082-93.
15. Jones DH. Ley S, Aitken A. Isoforms of 14-3-3 protein can form homo- and heterodimers in vivo and in vitro: implications for function as adapter proteins. FEBS Lett. 1995;368(1):55–8.
16. Yaffe MB. How do 14-3-3 proteins work?– Gatekeeper phosphorylation and the molecular anvil hypothesis. FEBS Lett. 2002;513(1):53–7.
17. Yang X. Qian K. Protein O-GlcNAcylation: emerging mechanisms and functions. Nat Rev Mol Cell Biol. 2017;18(7):452 – 65.
18. Veisova D. Rezabkova L, Stepanek M. Novotna P, Herman P. Vecer J, *et al.* The C-terminal segment of yeast BMH proteins exhibits different structure compared to other 14-3-3 protein isoforms. Biochemistry. 2010;49(18):3853-61.
19. Guo J. Dai S, Li H. Liu A, Liu C. Cheng D, *et al.* Identification and Expression Analysis of Wheat TaGF14 Genes. Front Genet. 2018;9:12.
20. Tian AL. Lu M, Calderón-Mantilla G. Petsalaki E, Dottorini T. Tian X, *et al.* A recombinant Fasciola gigantica 14-3-3 epsilon protein (rFg14-3-3e) modulates various functions of goat peripheral blood mononuclear cells. Parasit Vectors. 2018;11(1):152.
21. Kafle A. Puchadapirom P, Plumworasawat S. Dontumprai R, Chan-On W. Buates S, *et al.* Identification and characterization of protein 14-3-3 in carcinogenic liver fluke Opisthorchis viverrini. Parasitol Int. 2017;66(4):426–31.
22. Trujillo-Ocampo A. Cázares-Raga FE, *Del* Angel RM, Medina-Ramírez F. Santos-Argumedo L, Rodríguez MH, et al Participation of 14-3-3ε and 14-3-3ζ proteins in the phagocytosis, component of cellular immune response, in Aedes mosquito cell lines. Parasit Vectors. 2017;10(1):362.
23. Inamdar SM. Lankford CK, Laird JG. Novbatova G, Tatro N. Whitmore SS, *et al.* Analysis of 14-3-3 isoforms expressed in photoreceptors. Exp Eye Res. 2018;170:108–16.
24. Rivero G. Aldana AA, Frontini Lopez YR. Liverani L, Boccacini AR. Bustos DM, *et al.* 14-3-3ε protein-immobilized PCL-HA electrospun scaffolds with enhanced osteogenicity. J Mater Sci Mater Med. 2019;30(9):99.

25. Xue D. Xue Y, Niu Z. Guo X, Xu C. Expression analysis on 14-3-3 proteins in regenerative liver following partial hepatectomy. Genet Mol Biol. 2017;40(4):855–59.
26. Jiang H. Yu Y, Liu S. Zhu M, Dong X. Wu J, *et al.* Proteomic Study of a Parkinson's Disease Model of Undifferentiated SH-SY5Y Cells Induced by a Proteasome Inhibitor. Int J Med Sci. 2019;16(1):84–92.
27. Krzyzanowska A. García-Consuegra I, Pascual C. Antequera D, Ferrer I. Carro E. Expression of regulatory proteins in choroid plexus changes in early stages of Alzheimer disease. J Neuropathol Exp Neurol. 2015;74(4):359–69.
28. Smani D. Sarkar S, Raymick J. Kanungo J, Paule MG. Gu Q. Downregulation of 14-3-3 proteins in a kainic acid-induced neurotoxicity model. Mol Neurobiol. 2018;55(1):122–29.
29. Boyd JG. Smithson LJ, Howes D. Muscedere J, Kawaja MD, *Canadian Critical Care Translational Biology Group*. Serum proteomics as a strategy to identify novel biomarkers of neurologic recovery after cardiac arrest: a feasibility study. Intensive Care Med Exp. 2016;4(1):9.
30. Liang S. Xu Y, Shen G. Liu Q, Zhao X. Xu Z, *et al.* Quantitative protein expression profiling of 14-3-3 isoforms in human renal carcinoma shows 14-3-3 epsilon is involved in limitedly increasing renal cell proliferation. Electrophoresis. 2009;30(23):4152–62.
31. Aghazadeh Y. Papadopoulos V. The role of the 14-3-3 protein family in health, disease, and drug development. Drug Discov Today. 2016;21(2):278–87.
32. Leal MF. Ribeiro HF, Rey JA. Pinto GR, Smith MC. Moreira-Nunes CA, *et al.* YWHAE silencing induces cell proliferation, invasion and migration through the up-regulation of CDC25B and MYC in gastric cancer cells: new insights about YWHAE role in the tumor development and metastasis process. Oncotarget. 2016;7(51):85393–410.
33. Yang YF. Lee YC, Wang YY. Wang CH, Hou MF. Yuan SF. YWHAE promotes proliferation, metastasis, and chemoresistance in breast cancer cells. Kaohsiung J Med Sci. 2019;35(7):408–16.
34. Ferreira J. Félix A, Lennerz JK. Oliva E. Recent advances in the histological and molecular classification of endometrial stromal neoplasms. Virchows Arch. 2018;473(6):665–78.
35. Cotzia P. Benayed R, Mullaney K. Oliva E, Felix A. Ferreira J, *et al.* Undifferentiated uterine sarcomas represent under-recognized high-grade endometrial stromal sarcomas. Am J Surg Pathol. 2019;43(5):662–69.
36. L'Espérance S. Popa I, Bachvarova M. Plante M, Patten N. Wu L, *et al.* Gene expression profiling of paired ovarian tumors obtained prior to and following adjuvant chemotherapy: molecular signatures of chemoresistant tumors. Int J Oncol. 2006;29(1):5–24.
37. Sun Y. Xiaoyan H, Yun L. Chaoqun L, Jialing W. Liu Y, *et al.* Identification of key candidate genes and pathways for relationship between ovarian cancer and diabetes mellitus using bioinformatical analysis. Asian Pac J Cancer Prev. 2019;20(1):145–55.
38. Zhu YF. Gao GL, Tang SB. Zhang ZD, Huang QS. Effect of WFDC 2 silencing on the proliferation, motility and invasion of human serous ovarian cancer cells in vitro. Asian Pacific J Tropical Med, 2013, 6(4): 265 – 72.

39. Zhou Y. Fu X, Guan Y. Gong M, He K. Huang B. 1,3-Dicaffeoylquinic acid targeting 14-3-3 tau suppresses human breast cancer cell proliferation and metastasis through IL6/JAK2/PI3K pathway. Biochem Pharmacol. 2020;172:113752.
40. Li J. Xu H, Wang Q. Wang S, Xiong N. 14-3-3ζ promotes gliomas cells invasion by regulating Snail through the PI3K/AKT signaling. Cancer Med. 2019;8(2):783–94.
41. Zhou R. Shao Z, Liu J. Zhan W, Gao Q. Pan Z, *et al.* COPS5 and LASP1 synergistically interact to downregulate 14-3-3σ expression and promote colorectal cancer progression via activating PI3K/AKT pathway. Int J Cancer. 2018;142(9):1853–64.

Tables

Table 1. Expression of YWHAE in different ovarian tissues

Groups	Cases	Low		High		Positive Rate (%)	High expression Rate (%)
		-	+	++	+++		
Malignant	105	4	27	36	38	96.19%#	70.48%*
Borderline	24	14	6	2	2	41.67%	16.67%
Benign	18	15	1	2	0	16.67%	11.11%
Normal	16	15	1	0	0	6.25%	0

Table 2. Relationships between the expression of YWHAE and clinicopathological parameters

Groups	Cases	Low		High		Positive rate (%)	*P*-value	High expression rate (%)	*P*-value
		(-)	(+)	(++)	(+++)				
Age at diagnosis									
<55	54	4	13	18	19	93.0%	*P*=0.066	68.52%	*P*=0.651
≥55	51	0	14	18	19	100.0%		72.55%	
Pathological type									
Serous	71	2	14	28	27	97.0%	*P*=0.222	77.46%	*P*=0.073
Mucinous	7	1	3	2	1	86.0%		42.86%	
Endometrioid	19	1	6	4	8	95.0%		63.16%	
Clear cell carcinoma	8	0	4	2	2	100.0%		50.0%	
FIGO stage									
I-II	44	3	16	12	13	93.0%	*P*=0.307	56.82%	*P*=0.009
III-IV	61	1	11	24	25	98.0%		80.33%	
Differentiation									
Well and Moderate	51	3	13	12	23	94.0%	*P*=0.354	68.63%	*P*=0.687
Poor	54	1	14	24	15	98.0%		72.22%	
Lymphatic metastasis									
No	64	4	18	22	20	94.0%	*P*=0.310	65.63%	*P*=0.214
Yes	28	0	6	10	12	100.0%		78.57%	
Unknown[a]	13	0	3	4	6	100.0%		76.92%	

[a] 13 patients without lymphadenectomy

Table 3. Correlation between YWHAE and HE4 in ovarian cancer

(Sperman correlation coefficient Rs= 0.277, *P*=0.013)

YWHAE	HE4		case
	-	+	
-	0	3	3
+	9	68	77
Cases	9	71	80

Table 4. Linear regression analysis of YWHAE and HE4

	YWHAE score				HE4 score			
	Univariate		Multivariate		Univariate		Multivariate	
	β	*P*	β	*P*	β	*P*	β	*P*
HE4 score	0.307	0.009	0.307	0.009[a]				
YWHAE score					0.272	0.009	0.235	0.025[b]
Age at diagnosis	-0.238	0.772			0.137	0.859		
FIGO stage	1.429	0.087			1.772	0.023	1.436	0.062
Differentiation	-0.203	0.809			0.139	0.861		
Lymphatic metastasis	-0.017	0.986			1.383	0.118		

[a]represents multi-factor linear regression analysis, with YWHAE score as a variable, HE4 score as an argument;

[b]represents multi-factor linear regression analysis, with HE4 score as a variable, with YWHAE score and FIGO stage as arguments.

Figures

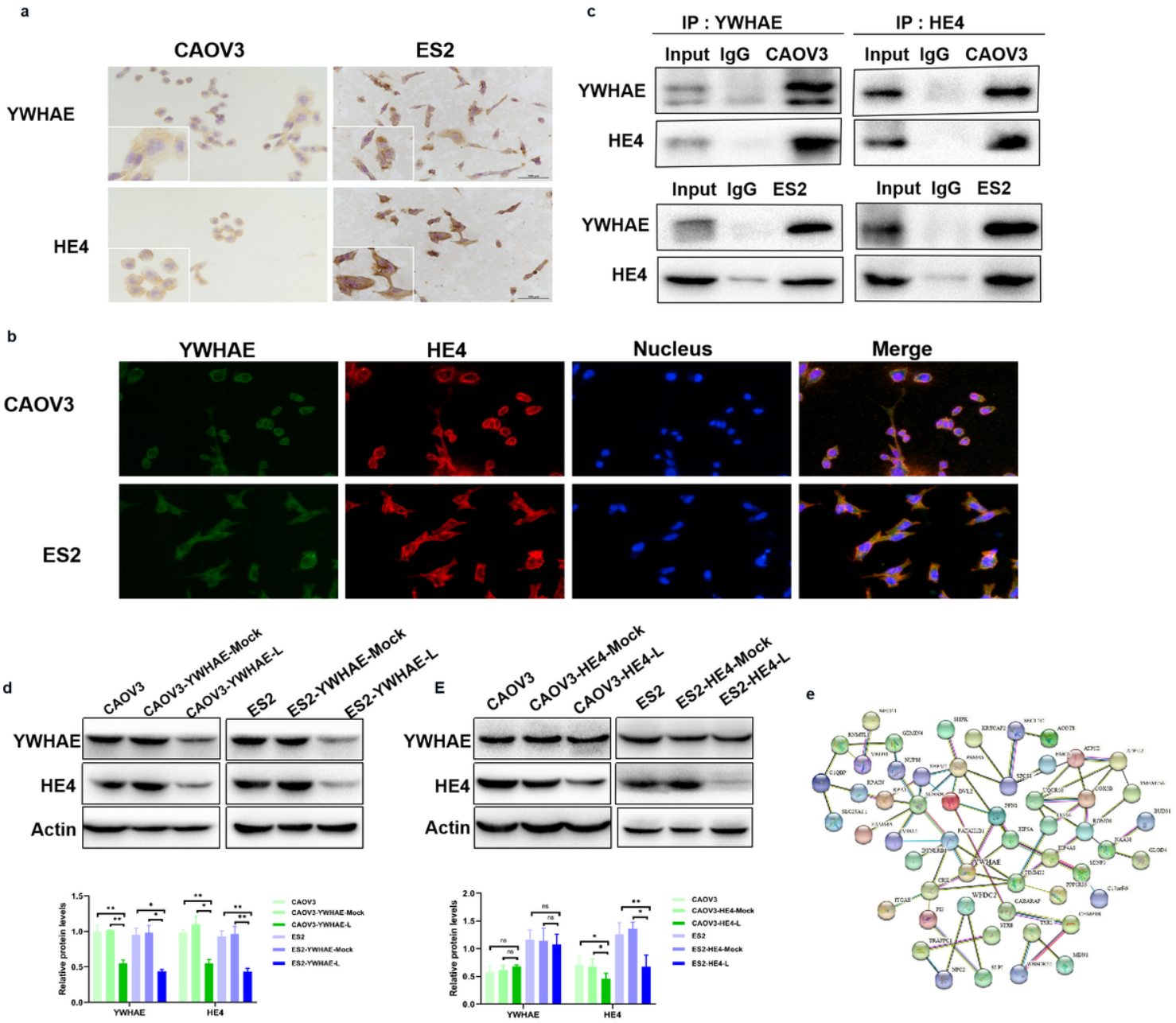

Figure 1

YWHAE and HE4 are interacting proteins in ovarian cancer a Expressions of YWHAE and HE4 in CAOV3 and ES2 cell; b Immunofluorescence test to detect the co-localization of YWHAE and HE4; c COIP detected the interaction between YWHAE and HE4 in CAOV3 and ES2 cell lines; d Western blot detected the regulation relationship between YWHAE and HE4; e HE4 acted as an interaction factor of YWHAE in bioinformatics.

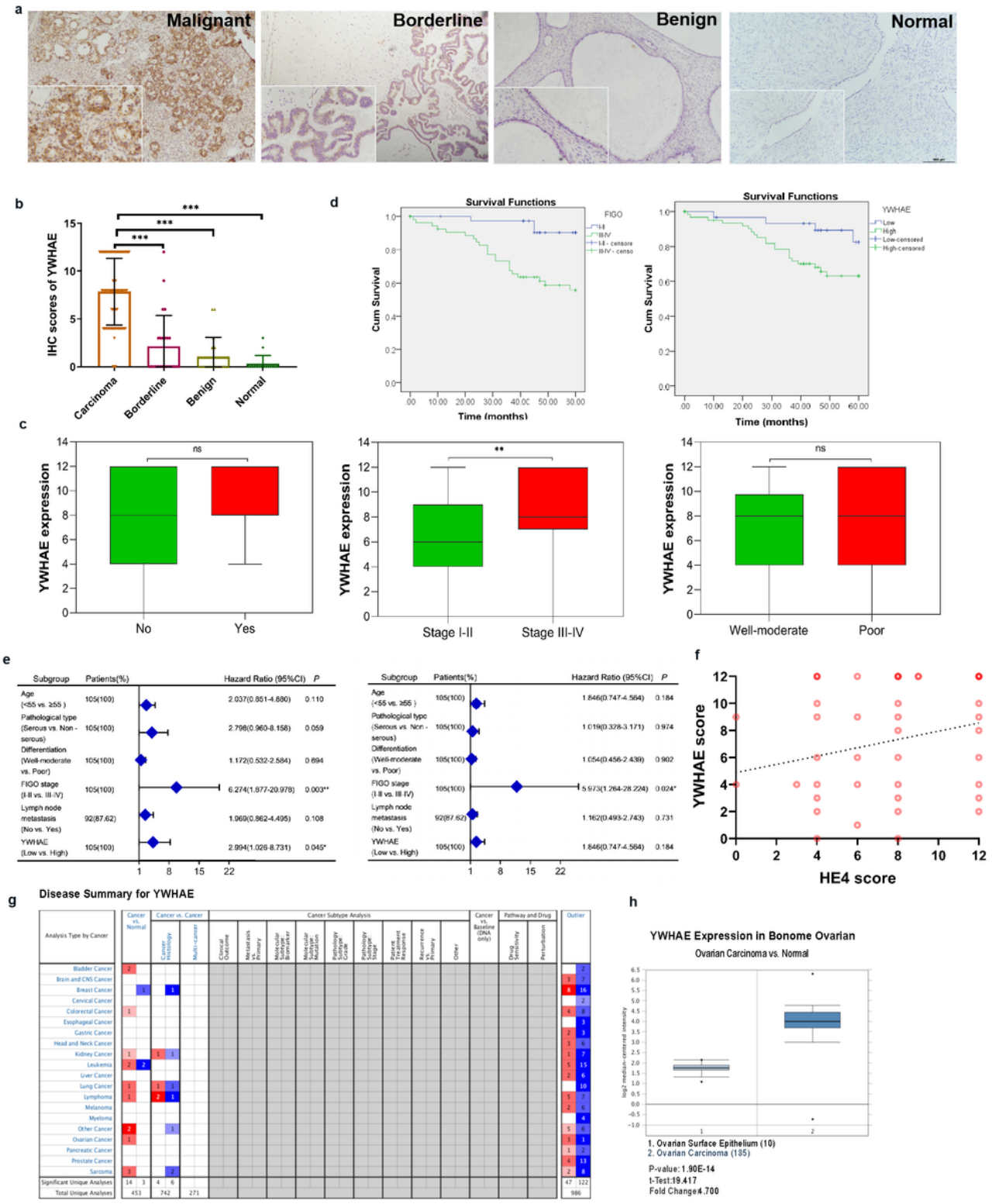

Figure 2

YWHAE expression in clinical specimens A The expressions of YWHAE and HE4 in the same position in malignant, borderline, benign and normal tissues; b YWHAE scores in different ovarian tissues; c Relationships between the expression of YWHAE, FIGO stage and differentiation; d The influence of FIGO stage and YWHAE on the survival and prognosis of ovarian cancer; e Univariate and multivariate Cox

analysis of different clinicopathological parameters of ovarian cancer; f Linear correlation between YWHAE and HE4 in ovarian cancer; g,h YWHAE expression in Oncomine database.

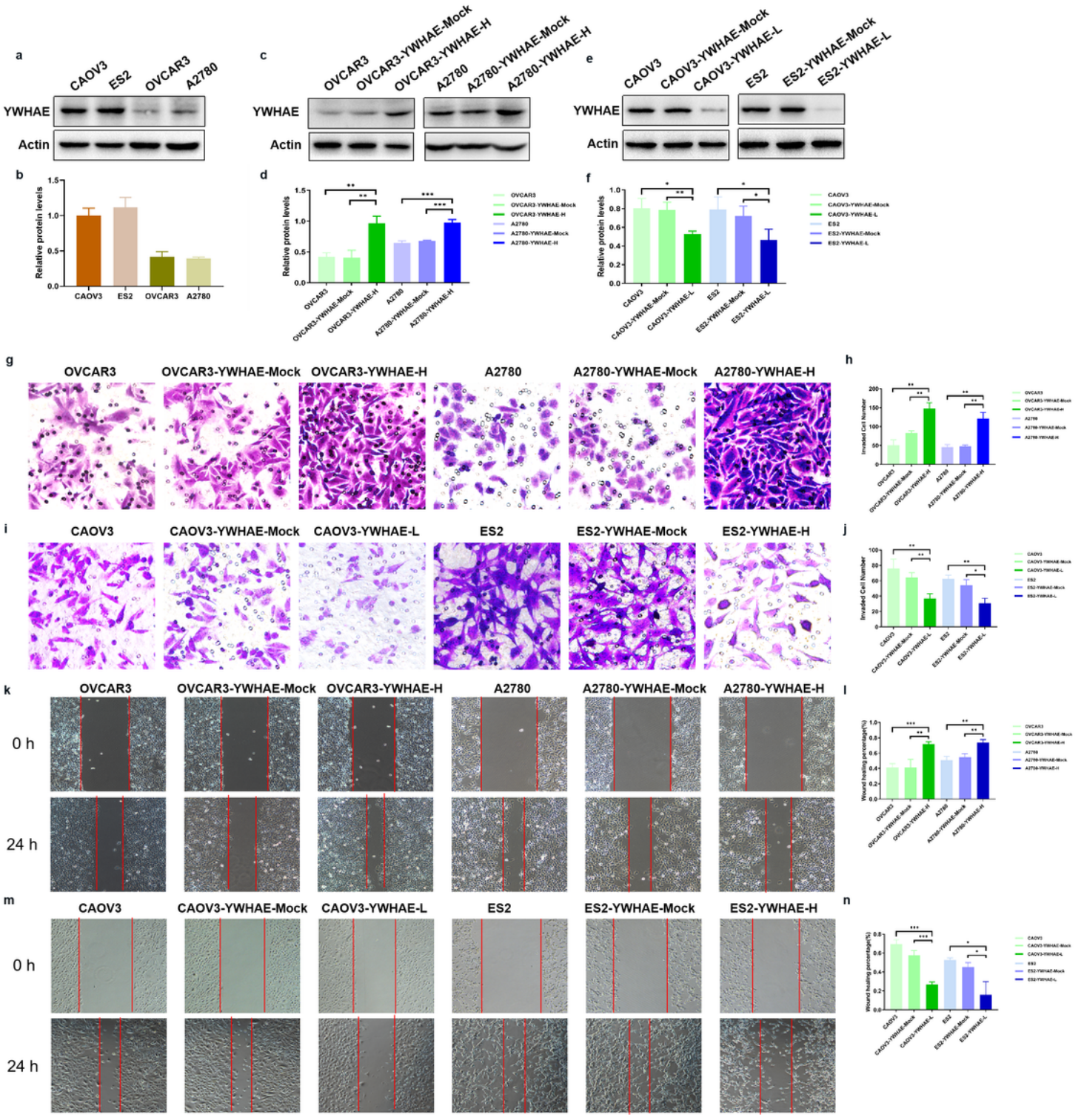

Figure 3

YWHAE affected cell invasion, migration and epithelial-mesenchymal transitionin ovarian cancer. a,b YWHAE expression in ovarian cancer cell line; c,d Western blot in YWHAE-high expression groups, mock-transduced groups and untransduced groups of OVCAR3 and A2780 cells; e,f Western blot in YWHAE-low

expression groups, mock-transduced groups and untransduced groups of CAOV3 and ES2 cells; g,h Effects of high expression of YWHAE on the invasion of ovarian cancer in OVCAR3 and A2780 cells; i,j Effects of low expression of YWHAE on the invasion of ovarian cancer in CAOV3 and ES2 cells; k,l Effects of high expression of YWHAE on the migration of ovarian cancer in OVCAR3 and A2780 cells; m,n Effects of low expression of YWHAE on the migration of ovarian cancer in CAOV3 and ES2 cells.

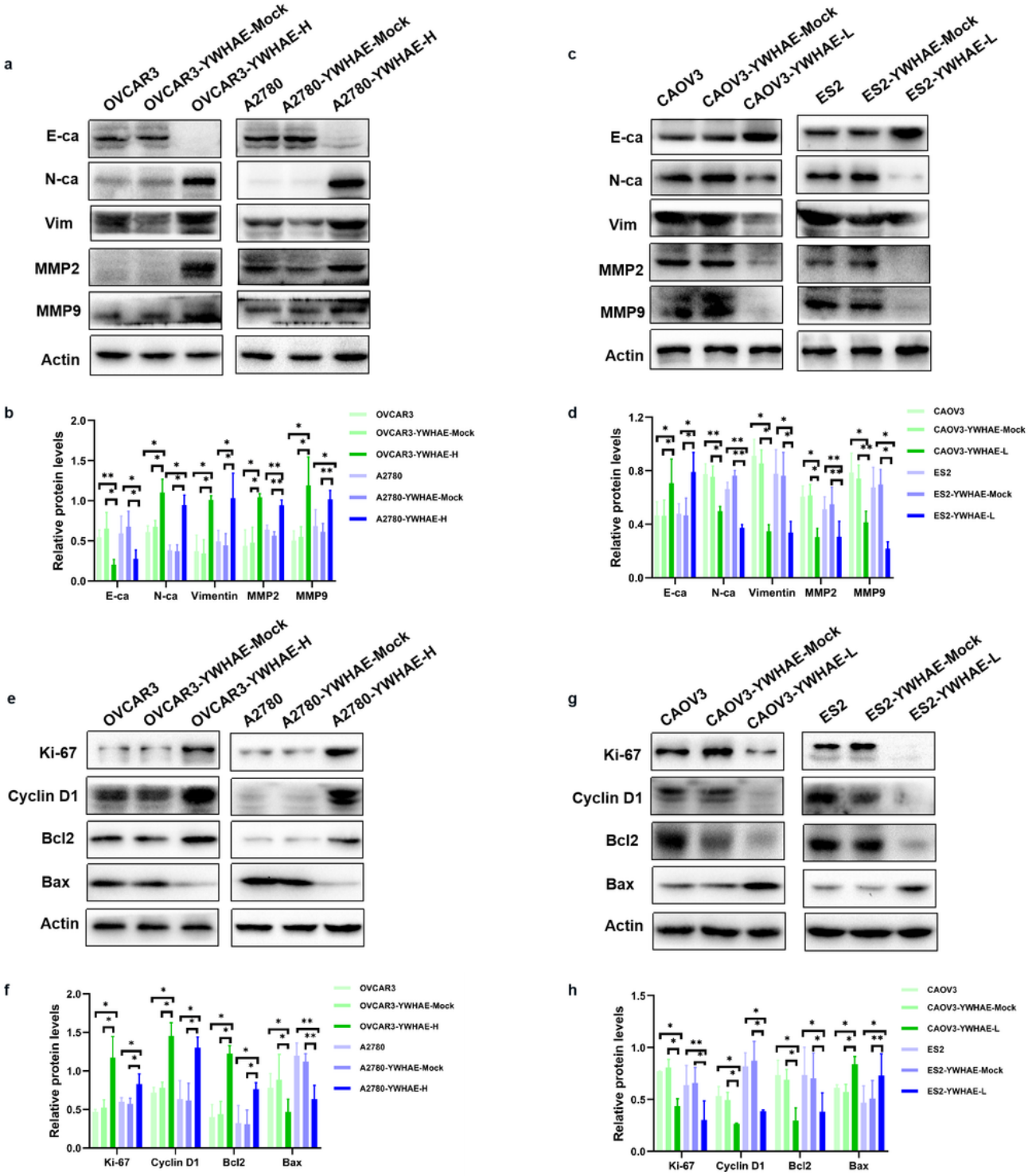

Figure 4

Western blot analysis of related proteins in ovarian cancer cells. a-d Expression of E-Cadherin, N-Cadherin, Vimentin, MMP2, MMP9 in ovarian cancer cells in high expression and low expression of YWHAE, respectively; e-h Expression of Ki67, Cyclin D, Bcl-2 and Bax in ovarian cancer cells in high expression and low expression of YWHAE, respectively.

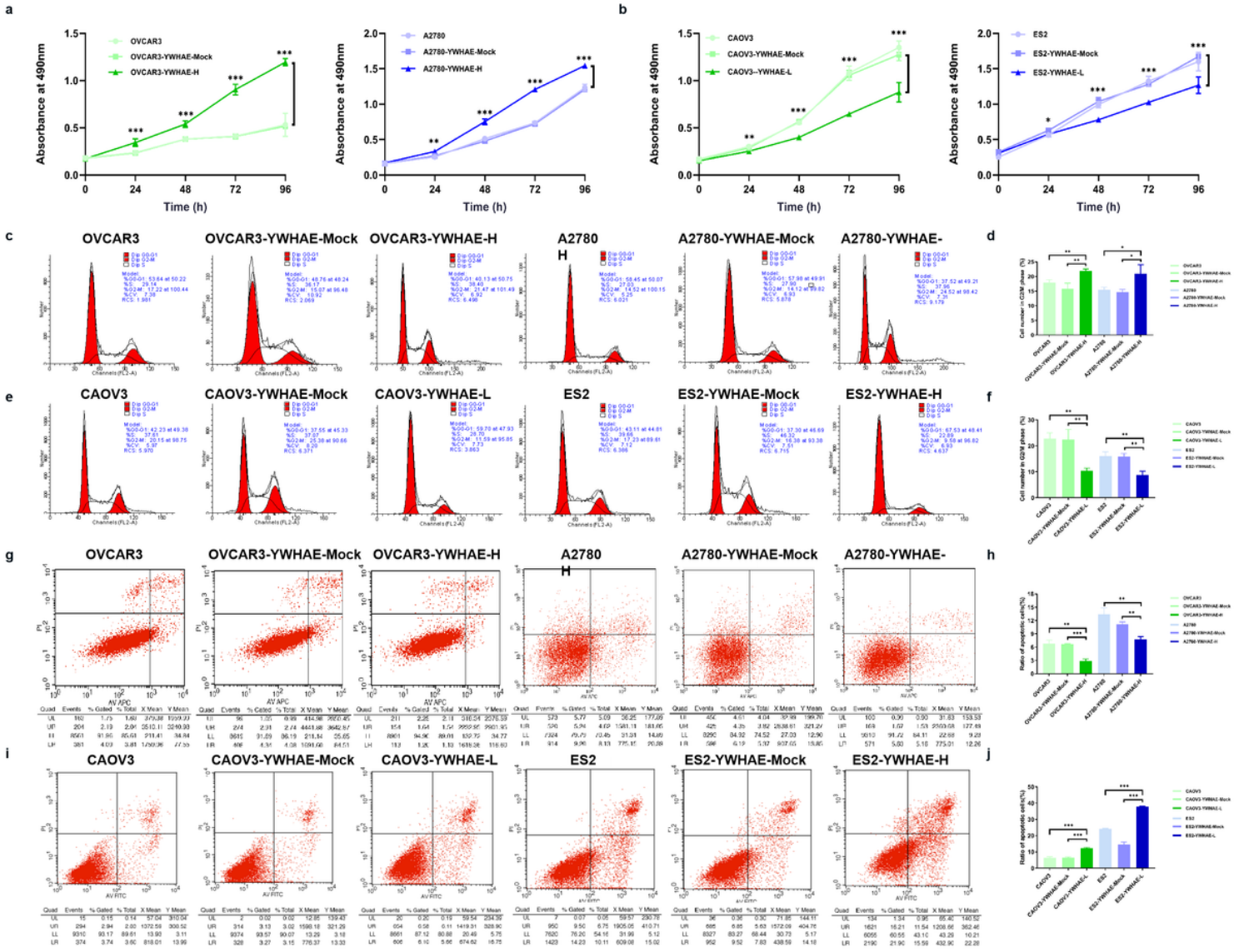

Figure 5

The influences of YWHAE on proliferation, apoptosis and cell cycle in ovarian cancer cells. a Overexpression of YWHAE promoted cell proliferation of ovarian cancer cells in MTT assay in OVCAR3 and A2780 cell lines; b YWHAE-siRNA inhibited cell proliferation of ovarian cancer cells in MTT assay in CAOV3 and ES2 cell lines; c,d Ovarian cells passed into G2/M phases after YWHAE overexpression; e,f G0/G1 phase arrested after YWHAE siRNA transfection; g,h YWHAE overexpression decreased the cell apoptosis in OVCAR3 and A2780 cell lines; i,j YWHAE-siRNA increased apoptosis of CAOV3 and ES2 cell lines.

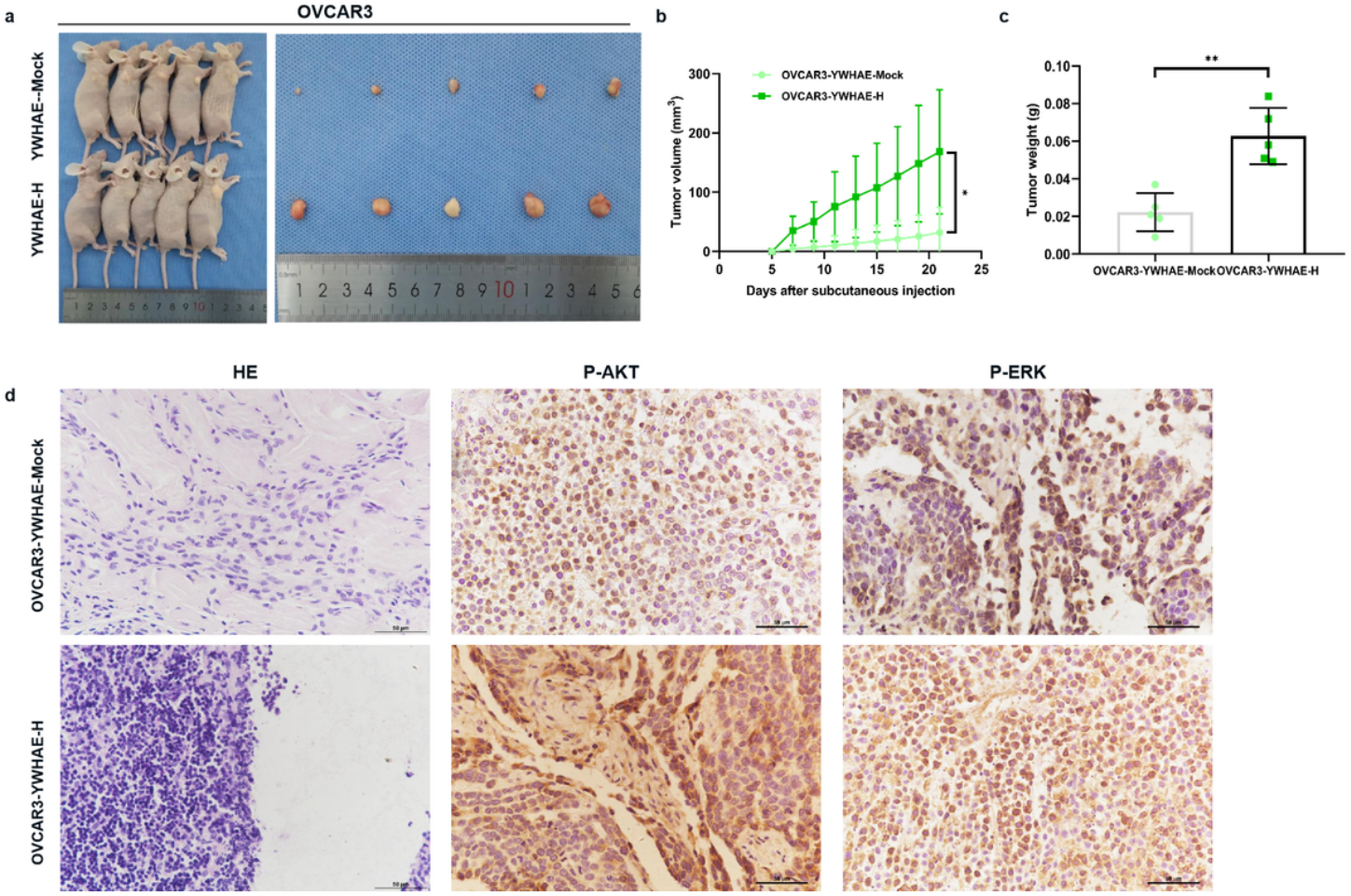

Figure 6

The impact of YWHAE on tumor formation and proliferation ability in vivo. a Subcutaneous xenograft of nude mice model was performed using YWHAE stable overexpression OVCAR3 cells; b,c Volume and quality changes of tumors;d Hematoxylin-Eosin staining, immunohistochemical staining of p-AKT and p-ERK in YWHAE-overexpressed group and control group.

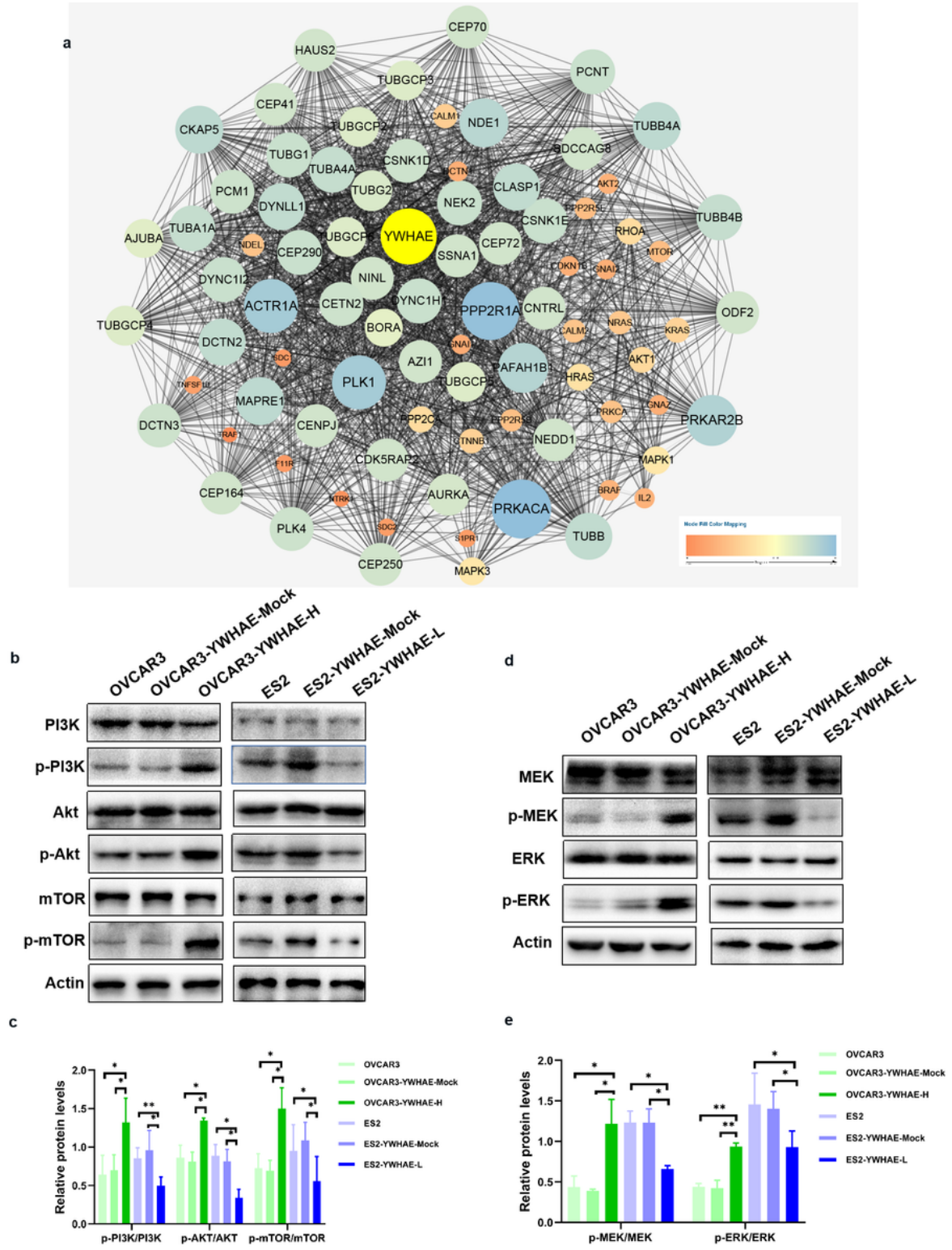

Figure 7

YWHAE-induced cellular effects by PI3K/AKT and MAPK signalling pathways a STRING database predicted the relevant molecules of YWHAE by PPI; b,c Expression of p-PI3K, PI3K, p-AKT, AKT, mTOR, p-m-TOR in ovarian cancer cells in high expression and low expression of YWHAE; d,e Expression of p-ERK, ERK, p-MEK, MEK in ovarian cancer cells in high expression and low expression of YWHAE.

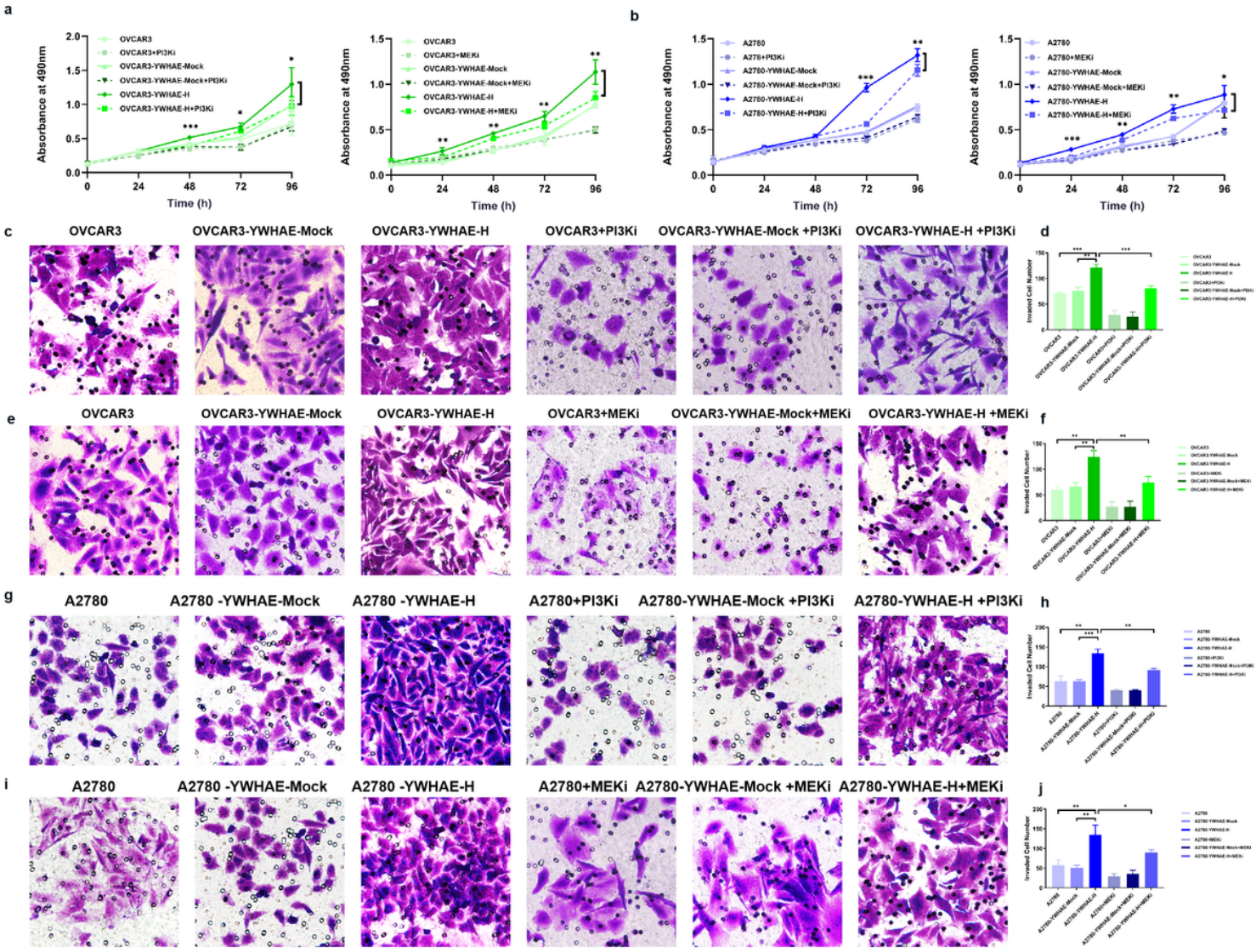

Figure 8

PI3K and MEK inhibitors reduce MTT and invasion abilities in ovarian cancer cells. a,b PI3K and MEK inhibitors reduce proliferation ability in YWHAE-high expression groups, mock-transduced groups and untransduced groups of OVCAR3 and A2780 cells; c-j PI3K and MEK inhibitors reduce invasion ability in YWHAE-high expression groups, mock-transduced groups and untransduced groups of OVCAR3 and A2780 cells.

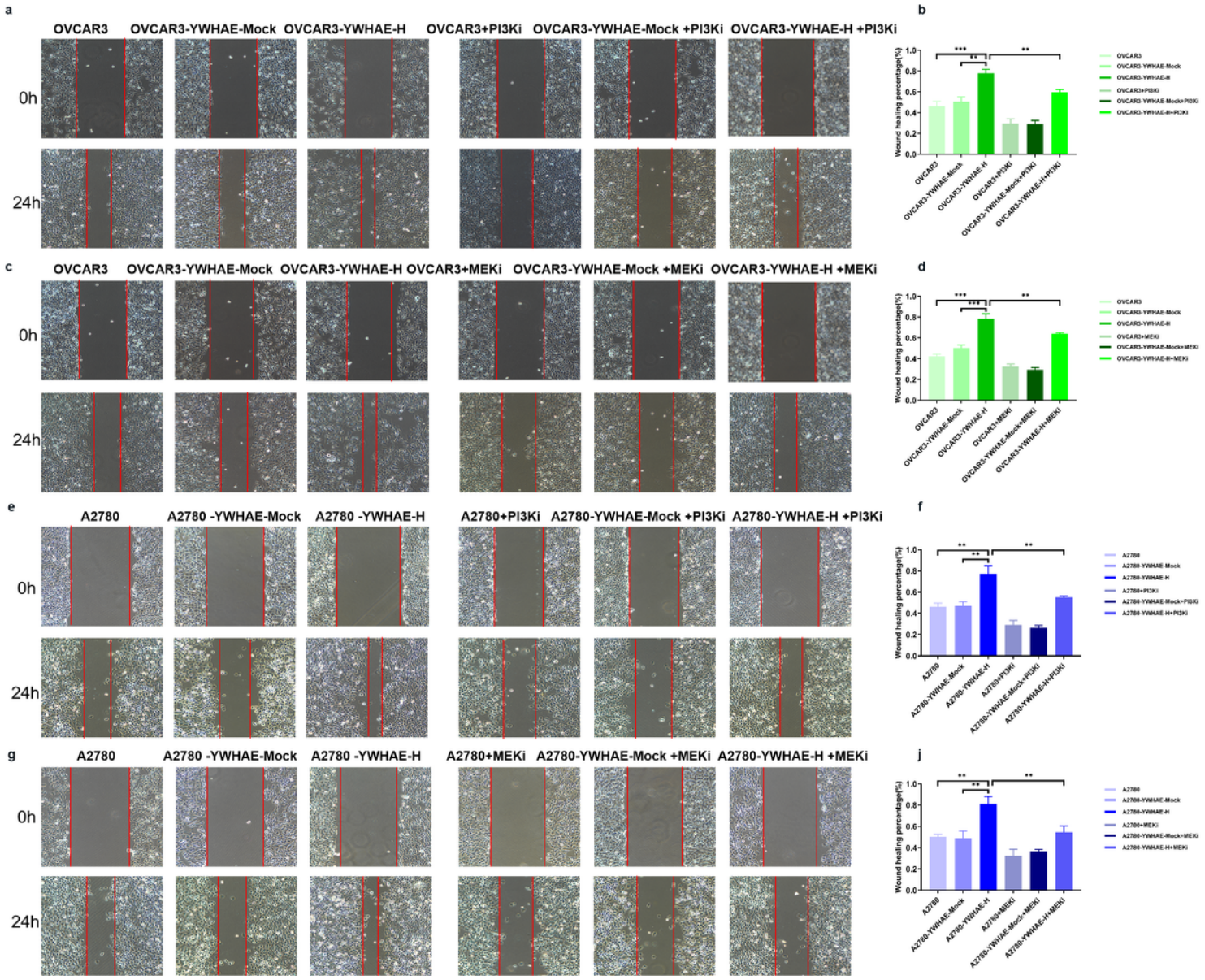

Figure 9

PI3K and MEK inhibitors reduce migration ability in ovarian cancer cells.